Design and Improvement of Airborne Ocean Radar Fault Detection Algorithm

Liang Pang(✉)

Public Basic Course Department, Wuhan Institute of Design and Sciences, Wuhan 430025, China
pangliang0611@163.com

Abstract. Fault detection can ensure the safe operation of airborne ocean radar. In order to improve the fault detection performance of airborne ocean radar, the design and improvement of the fault detection algorithm for airborne ocean radar is proposed. Based on the current and voltage values of stable operation, the fault area is determined. The fault information is decomposed by wavelet transform, the fault information is reconstructed, and the fault location is determined. Through the preprocessing of the fault data, the feature matching degree of the fault data is defined, and the features of the fault data are extracted by using the information state function of the fault data. Calculate the average trajectory of the observation vector of the operating state, and combine the operating trajectories of the fault data variables at different times to detect the faults of airborne ocean radar. The experimental results show that the algorithm in this paper has certain effectiveness in detecting the faults of airborne ocean radar, and has better performance in terms of missed detection rate, false detection rate and signal-to-noise ratio of fault signal acquisition.

Keywords: Fault Detection · Airborne Ocean Radar · Fault Location · Feature Extraction · Area Determination

1 Introduction

The airborne marine radar uses a laser with a high perspective in the water as the pulse emission source, which has the advantages of mature technology, large transmission power, small size, etc., and can detect the sound speed and temperature of the marine boundary layer in a large area [1, 2]. The airborne marine radar will inevitably fail in the process of operation. Once an airborne ocean radar fails, it will output incorrect conservation monitoring information, seriously affecting the operation of the ocean exploration system, and even causing significant economic losses. Therefore, the fault detection of airborne Marine radar equipment has become a key research topic.

Wang Liangcheng et al. [3] considered that the existing methods could not complete the conversion of non-linear drive information, resulting in the low fault detection rate of motor drive system, and a method of fault detection of motor drive system under PLC technology is proposed. The frequency band components of the drive motor are

L. Yun et al. (Eds.): ADHIP 2023, LNICST 548, pp. 116–131, 2024.
https://doi.org/10.1007/978-3-031-50546-1_8

obtained by wavelet packet analysis, and the fault characteristic parameters are extracted by analyzing the changes of each frequency band component. According to the fault characteristics, under the PLC technology, the non-linear information of the motor drive fault characteristic parameters is converted into linear information by combining the kernel method and the principal component analysis method. Finally, the fuzzy kernel clustering method is used to cluster the linearized information to complete the fault detection of the motor drive system. The experimental results show that this method can realize the motor fault detection. However, the signal to noise ratio of fault signal acquisition is low. Bao Haibo et al. [4] proposed a static voltage stability fault screening and ranking method considering the uncertainty of power generation in order to effectively analyze the impact of power system equipment faults and uncertainty of power generation on system static voltage stability. A deterministic voltage stability critical point model under N-1 fault scenario is established, and the severe fault set is screened according to the obtained load margin after fault.Considering the random distribution of wind power and photovoltaic power generation, a voltage stability probability evaluation model under fault scenarios is established, and the stochastic response surface method is used to obtain the cumulative probability distribution of load margins in fault scenarios. The two types of post-failure systems are sorted for voltage stability and classified according to the accumulated probability of the load margin. The calculation results of the IEEE 118 node standard system show that the proposed fault screening and sorting method is effective, and it can screen and sort the probabilistic static voltage stability of the system under each fault scenario, that is, faults is detected, but the method has a high missed detection rate. Reference [5] proposed a fault diagnosis method based on immune algorithm (Immune Algorithm, IA) for the problem of low diagnostic efficiency of traditional fault diagnosis methods for hydro-generator units. The collected fault sample data of the hydro-generator unit is preprocessed to form the fault type code, and the relevant parameters of the algorithm are set. On this basis, the immune algorithm program developed by MATLAB is used to predict the fault. This method has the advantages of simple operation and easy capacity expansion, etc., but its false detection rate is high. Reference [6] in response to the problem of low accuracy and long recognition time caused by the lack of preprocessing of fault data in LiDAR hardware, a research method for pattern recognition of LiDAR hardware fault data is proposed. Wavelet transform is used to analyze noise data, obtain data features, and shorten fault recognition time; Perform fusion processing on high-dimensional feature data, extract association rule feature quantities of fault data for fault diagnosis and recognition. However, in the process of obtaining fault data features, there is a problem of weak continuity of fault signals. Reference [7] aiming at the problems of intermittent faults and comprehensive performance degradation of airborne radar, an early warning technology considering degradation and intermittent faults is proposed. By analyzing the principle of radar fault detection, a test Index set is set up. Apply the NDGM model to clarify the fault warning decision-making process, analyze the growth of small wave energy spectrum entropy in the decision-making process, detect the operating status of radar components, and identify fault information, however, in the process of detecting the operating status of the radar, the integrity of the status data cannot be guaranteed, resulting in low accuracy of fault detection.

Based on the above research background, a fault detection method for airborne marine radar is designed in this paper to ensure the safe operation of airborne marine radar.

2 Airborne Marine Radar Fault Detection

The overall structure of airborne marine radar fault detection is shown in Fig. 1.

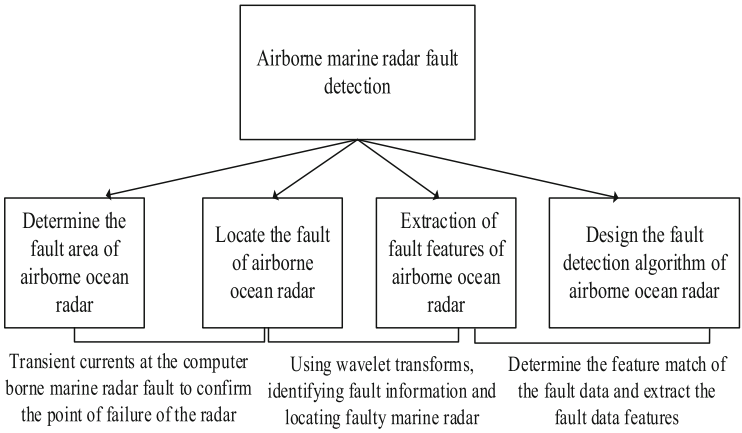

Fig. 1. Airborne marine radar fault detection architecture

2.1 Determine the Fault Area of Airborne Ocean Radar

When the airborne ocean radar fails, the current and voltage values around the fault point will change, so the transient current at the fault of the airborne ocean radar can be expressed as:

$$I_z + I_f = -I_f \frac{Z_1}{Z_1 + Z_2} \tag{1}$$

where, I_z represents the transient current at the fault location of the airborne ocean radar, I_f represents the current reflected wave at the fault of the airborne ocean radar, Z_1 represents the reflected wave impedance of the airborne ocean radar fault, and Z_2 represents the incident wave of the airborne ocean radar fault. Impedance.

The intra class aggregation degree of fault data of airborne ocean radar is calculated by using the transient current at the fault of airborne ocean radar. The formula is:

$$L_W^{(k)} = \sum_{i=1}^{M} L_i^{(k)} \tag{2}$$

where, M represents the number of categories of airborne ocean radar fault data, and $L_i^{(k)}$ is the aggregation degree of the k-dimensional airborne ocean radar fault data attribute belonging to the i category, which can be calculated by the following formula:

$$L_i^{(k)} = \sum_{x \in G_i} \left(X^{(k)} - Q_i^{(k)} \right)^2 \tag{3}$$

where, $X^{(k)}$ represents the attribute vector of the k-dimensional airborne ocean radar fault data, G_i represents the sample of the airborne ocean radar fault data in category i, and $Q_i^{(k)}$ represents the attribute vector of the k-dimensional airborne ocean radar fault data in category i.

When the airborne ocean radar is running stably, based on the current and voltage values during the operation, according to the degree of intra-class aggregation of the airborne ocean radar fault data, the fault area of the airborne ocean radar is determined. The principle is shown in Fig. 2.

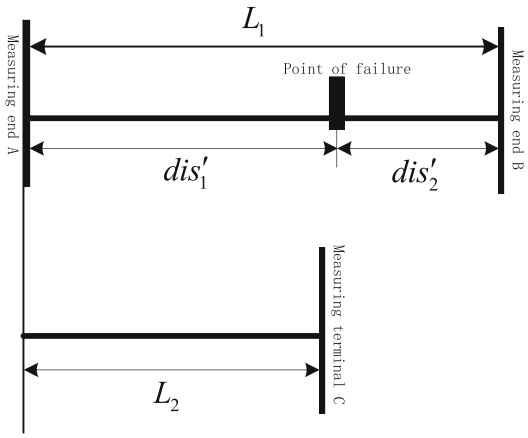

Fig. 2. Principle of determining the fault area of airborne ocean radar

If the fault location of airborne ocean radar is defined as Ω, the two fault points located by airborne ocean radar are L_1 and L_1 respectively. Install the transient current detection device on the l_1 terminal of the airborne ocean radar, and set A and B as two measurement terminals; install the voltage detection device on the ζ_1 of the airborne ocean radar, dis_1' and dis_2' represent the fault point Ω to the measurement The straight-line distance between ends A and B. Assuming that the transient current I is constant, then:

$$\begin{cases} I(T_1 - T_0) = dis_1' \\ I(T_2 - T_0) = dis_2' \\ I(t_3 - t_0) = L_2 + dis_1' \\ dis_1 + dis_2 = L_1 \end{cases} \tag{4}$$

It is obtained that the fault point Ω of airborne ocean radar is in the area of the fault line according to the above process. The calculation result is:

$$dis_1 = \frac{L_1}{2} + \frac{L_2(T_1 - T_2)}{2(T_3 - T_1)} \tag{5}$$

The fault area of airborne ocean radar is determined according to the above calculation process.

2.2 Locate the Fault of Airborne Ocean Radar

Wavelet transform is used to convert the fault information of airborne ocean radar in order to locate the fault of airborne ocean radar complete the effective identification of the fault information, and finally realize the accurate location of the fault of airborne ocean radar.

The wavelet function is used to collect the fault data of the airborne ocean radar, and the state function of the fault information of the airborne ocean radar is obtained, which is expressed as:

$$X_i = \frac{1}{p_j(k)} f_i(x_i, u_i) \tag{6}$$

where, $p_j(k)$ represents the posterior probability estimation of fault information of airborne ocean radar, $x_i \in R^n$ represents the feature state vector of fault information of airborne ocean radar, and $u_i \in R^m$ represents the feature of fault information of airborne ocean radar.

Assuming that $\phi(t)$ is a wavelet discrete function, the transformation function $\phi_{f,g}(t)$ obtained is:

$$\phi_{f,g}(t) = \frac{1}{\sqrt{f}} \phi\left(\frac{t-g}{f}\right) \tag{7}$$

where, f represents the wavelet transform factor, g represents the movement factor, $\phi_{f,g}(t)$ is obtained by the wavelet transform $\phi(t)$, and the wavelet transform function is obtained by performing the wavelet transform on f and g.

Let $s(t)$ be the fault signal of airborne ocean radar, according to formula (7), use $\phi(t)$ to perform discrete wavelet transform on $s(t)$, and obtain the coefficient of wavelet transform as:

$$T_s(f, g) = \frac{1}{\sqrt{f}} \int s(t) \phi^{\cdot}\left(\frac{t-g}{f}\right) dt \tag{8}$$

where, f, g and t represent constants in the process of wavelet transform. Therefore, formula (8) is a continuous wavelet transform signal, which can explain that the fault signal of airborne ocean radar is continuous.

Wavelet function is used to reconstruct the fault information of airborne ocean radar [8], any fault location $e(t)$ of airborne ocean radar can be expressed as:

$$e(t) = e_l(t) + T_s\left(2^l, 2^l t\right) \lambda_{l,v} \tag{9}$$

where, $e_l(t)$ represents the signal near the fault point of airborne ocean radar, $T_s\left(2^l, 2^l t\right)$ represents the discrete wavelet signal of the fault signal of airborne ocean radar under different fault conditions, and is expressed as:

$$T_s\left(2^l, 2^l t\right) = \frac{1}{\sqrt{2^l}} T_y(f, g) \tag{10}$$

where, l is the fault weight of airborne ocean radar under different fault conditions.

Let $\phi(t)$ be the wavelet basis function, then $\lambda_{l,v}$ is the wavelet coefficient of the fault location point of the adjacent airborne ocean radar, which can be decomposed into:

$$c_{l,v} = \left\langle e(t), \phi_{l,v}(t) \right\rangle \tag{11}$$

The fault information of airborne ocean radar under different fault conditions is reconstructed according to the wavelet coefficient of formula (11), and the accurate location of airborne ocean radar fault is obtained as follows:

$$e(t) = \sum_{l} \sum_{v} \beta_l \lambda_{l,v} \phi_{l,v}(t) \tag{12}$$

where, β_l represents the location information of the fault point of the airborne ocean radar.

The location of the fault of the airborne ocean radar is obtained according to the above process.

2.3 Extraction of Fault Features of Airborne Ocean Radar

It is necessary to preprocess the fault data, convert all the fault data into the mapping interval of [0, 1] in order to ensure the integrity of the fault data of airborne ocean radar, so as to eliminate the noise in the fault data of airborne ocean radar and reduce the interference of noise to the mining of fault data of airborne ocean radar. The following methods are used to preprocess the fault data of airborne ocean radar, which is expressed as:

$$z^* = \frac{z - \min(z)}{\max(z) - \min(z)} \tag{13}$$

where, z^* represents the preprocessed airborne ocean radar fault data, $\max(z)$ represents the maximum value existing in the airborne ocean radar fault data, and $\min(z)$ represents the minimum value existing in the airborne ocean radar fault data.

After preprocessing the fault data of airborne ocean radar, the regression equation of the fault data of airborne ocean radar is constructed, and the expression is as follows:

$$\left(m^*, n^*\right) = \zeta_1 \times \frac{a_1 m_1 + a_2 + m_2^* + a_p + m_p^*}{\lambda_1} \tag{14}$$

where, ζ_1 represents the composition of fault data, (m^*, n^*) represents the regression coefficient of fault data, a_1, a_2 and a_p represent the fault points with frequent fault data, and m_2^* and m_p^* respectively represent the correlation between frequent fault points.

Specific methods is used to approximate and linearly fit the fault data of airborne ocean radar. These methods do not affect its basic form, nor do they require saving the characteristics of fault data, and can also compress the characteristics of fault data, which will eventually cause faults. There are differences in the length of the data, so the fault data must be processed with the same length.

The fault data M and B N of airborne ocean radar are set as:

$$\begin{cases} M = \{(g_1, a_1), \cdots, (g_L, a_L)\} \\ N = \{(g_1, b_1), \cdots, (g_L, b_L)\} \end{cases} \tag{15}$$

Assuming that the lengths of fault data M and N of airborne ocean radar are equal, the fault data sequences SM and SN are matched, and the expressions are as follows:

$$\begin{cases} SM = \{(g_{x1}, a_{x1}), \cdots, (g_{xm}, a_{xm})\} \\ SN = \left\{\left(g_{y1}, b_{y1}\right), \cdots, \left(g_{yn}, b_{yn}\right)\right\} \end{cases} \tag{16}$$

where, the corresponding lengths of the fault data sequences SM and SN of the airborne ocean radar are m and n, respectively. The characteristic length of the fault data is quite different. Therefore, it cannot be linearly simulated by using the Euclidean distance and other metric formulas. Therefore, it is necessary to use the feature extraction algorithm to process the fault data of the airborne ocean radar in equal lengths, and obtain the equal length processing. The fault data of airborne ocean radar, namely:

$$\begin{cases} SM^* = \{(g_{l1}, a_{l1}), \cdots, (g_{ll}, a_{ll})\} \\ SN^* = \{(g_{l1}, b_{l1}), \cdots, (g_{ll}, b_{ll})\} \end{cases} \tag{17}$$

After equal length processing of fault data, the weight mapping matrix of fault data of airborne ocean radar is obtained, which is expressed as:

$$U(h) = \frac{\partial_p \times \Lambda^* \times \varepsilon(s)}{\Pi_i + f(\varsigma)} \times \ell(u) \tag{18}$$

where, ∂_p A represents the feature quantity of the airborne ocean radar in the normal operation state, Λ^* represents the fault data set of the airborne ocean radar, $\varepsilon(s)$ represents the total number of fault data sets, $f(\varsigma)$ represents the characteristic attribute of the fault data, and $\ell(u)$ represents the airborne ocean radar. A collection of feature items for fault data.

Combined with the principle of feature extraction, the feature matching degree of fault data of airborne ocean radar is defined, namely:

$$\zeta = \frac{1}{A \cdot \phi_p(q)} \sqrt{\sum_{l=1}^{A} \left| 1 - \frac{u_l}{k_l} \right|^2} \cdot \varphi_p(q) \tag{19}$$

where, $\varphi_p(q)$ represents the correlation between attribute q and fault data, $\phi_p(q)$ represents the non correlation between attribute q and fault data, A represents the number of airborne ocean radar, u_l represents the fault data set, and k_l represents the reliability of airborne ocean radar.

It is necessary to first use the time-frequency analysis method to extract the characteristics of the fault data of the airborne ocean radar in order to extract the characteristics of the fault data of the airborne ocean radar [9, 10], and the information function of the fault data of the airborne ocean radar is obtained as follows:

$$Z(x_i) = f(x_i, z_i)k_g(i) \tag{20}$$

where, $k_g(i)$ represents the characteristic value of the fault data of airborne ocean radar, x_i represents the characteristic state vector of the fault data of airborne ocean radar, and z_i represents the characteristic number of the fault data of airborne ocean radar.

The fault data of airborne ocean radar defines as $S(x_i)$, the feature preprocessing $S(x_i)$, and the transformed fault data as $\gamma(x_i)$, the following formula is used to extract the characteristics of the fault data of airborne ocean radar, which is expressed as:

$$T_r = \frac{S(x_i) + \gamma(x_i)}{W_g \times f_z} \times \lambda_d \tag{21}$$

where, W_g represents the feature quantity of fault data of airborne ocean radar, f_z represents the generation cycle of fault data features of airborne ocean radar, and λ_d represents the feature extraction location of fault data of airborne ocean radar.

The feature matching degree of the fault data is defined through the preprocessing of the airborne ocean radar fault data, and the characteristics of the airborne ocean radar fault data are extracted by using the information state function of the fault data.

2.4 Design the Fault Detection Algorithm of Airborne Ocean Radar

After the fault feature extraction of airborne ocean radar is completed, the fault detection method is designed, which is the last step of fault detection. In the process of detecting faults of airborne ocean radar, the observation vector of the operating state of airborne ocean radar is defined, and the expression is:

$$\tau = \frac{\xi u_f}{\chi_i * \Gamma_p} \cdot \alpha_e \tag{22}$$

where, ξ represents the operating state threshold of airborne ocean radar, u_f represents the number of pivots in the fault data of airborne ocean radar, χ_i represents the covariance matrix between the pivots, and Γ_p represents the failure of airborne ocean radar under normal conditions. Data, α_e represents the historical data of airborne ocean radar.

The observation vector of the operating state of airborne ocean radar is used as the key variable of fault detection. By analyzing the historical operation of airborne ocean radar, the average trajectory of the observation vector of the operating state is calculated, namely:

$$Z_r = \frac{Y_e + Y_p}{C_p} \cdot \sqrt{X_t + Y_i} \tag{23}$$

where, Y_e represents a single element in the trajectory of the key variable, Y_p represents the change trend information of the key variable during the operation time of the airborne ocean radar, C_p represents the dynamic characteristics of the key variable, and X_t

represents the variable value of the fault detection sample of the airborne ocean radar., Y_i represents the trajectory vector of the key variable.

In view of the high degree of electronization of airborne ocean radar, the requirements for the operation trajectory of fault variables are very strict. It is necessary to give the operation trajectory of fault data variables of airborne ocean radar at different times, namely:

$$E_t = \frac{x_p \cdot G_k}{\gamma_u} + \sigma_p \tag{24}$$

where, x_p represents the weight of the airborne ocean radar fault data in the trajectory operation space, G_k represents the trajectory judgment of the airborne ocean radar fault data, γ_u represents the sampling interval of the airborne ocean radar fault data, and σ_p represents the fault data of the same period. Similarity.

Assuming that $\{a_i\}$ and $\{b_i\}$ represent the fault signals during the operation of the airborne ocean radar, the fundamental frequency vibration of the operating signal of the airborne ocean radar can be obtained by using the following formula:

$$X_i(t) = \frac{f(x) \times [\{a_i\} \cdot \{b_i\}]}{S_j(t) \times x_{ij}} J_i(t) \tag{25}$$

where, $S_j(t)$ represents the fault signal of the j airborne ocean radar, x_{ij} represents the fault signal of $S_j(t)$ at the i measuring point, and $J_i(t)$ represents the detection factor.

When the airborne ocean radar has communication failure, it is difficult to ensure its normal operation, so it is necessary to extract the key variable information of the airborne ocean radar failure, namely:

$$R_p = \frac{f_p \cdot \phi_o}{f_u + \sigma_l} \tag{26}$$

where, f_p represents the type set of fault samples of airborne ocean radar, ϕ_o represents the score matrix of fault data of airborne ocean radar in the principal component space, f_u represents the trajectory trend diagram of detection variables of fault data of airborne ocean radar, and σ_l represents the trajectory vector of fault detection data samples of airborne ocean radar.

The airborne ocean radar faults is detected according to the key variable information of airborne ocean radar faults, namely:

$$J_r = \frac{n \mp \Phi_e}{C_p} \times \frac{Z_r}{R_p} \times E_t \tag{27}$$

where, n represents the number of key variables, and Φ_e represents the process data of the key variable information of airborne ocean radar failures.

To sum up, according to the running trajectories of the airborne ocean radar fault data variables at different times, the airborne ocean radar faults are detected.

3 Experimental Analysis

3.1 Experimental Environment

An experimental platform for fault detection is built in the matlab environment in order to verify the feasibility of the method in this paper in detecting faults of airborne ocean radar. The specific configuration of this experimental platform is shown in Table 1.

Table 1. Experimental platform configuration

Serial number	Name	Parameter
1	Operating system	64-bit Windows 7
2	Memory size	8 GB
3	Main frequency	3.6 GHz
4	Processor	Intel(R) Core(TM) i8–3770
5	Matlab version	2019 A

The experimental platform built in this paper is composed of 10 PCs and the operating environment of airborne ocean radar. The experimental data is collected when the airborne ocean radar is in a fault state. The fault of airborne ocean radar is detected using the methods in this paper and the traditional methods.

3.2 Collecting Fault Data Samples of Airborne Ocean Radar

The sampling block length is 1000 (experimental space), the sampling period for airborne ocean radar fault data is 0.05 s (experimental time), the number of iterations of fault data feature extraction is 50, and the number of fault data samples is 1200. In the process of equipment failure, first, the failure data samples of airborne ocean radar are collected according to the characteristics of the failure data, as shown in Fig. 3.

3.3 Detecting Faults of Airborne Ocean Radar

The sample data in Fig. 3 is taked as the test object, combined with the idea of feature fusion, the correlation of airborne ocean radar fault data is integrated, and under different fusion coefficients, the method in this paper is used to detect airborne ocean radar faults, and detection of airborne ocean radar faults. The output is shown in Fig. 4.

The fault data of airborne ocean radar can be detected by the method in this paper according to the results in Fig. 4. When the fusion coefficient is 0.2, the early detection output of fault data has changed. The reason is the difference in the matching degree of fault features in the early stage of fault detection. As a result, it began to stabilize afterwards; when the fusion coefficient was 0.4, the detection output of the fault data was relatively stable, which verifies the effectiveness of the method in this paper.

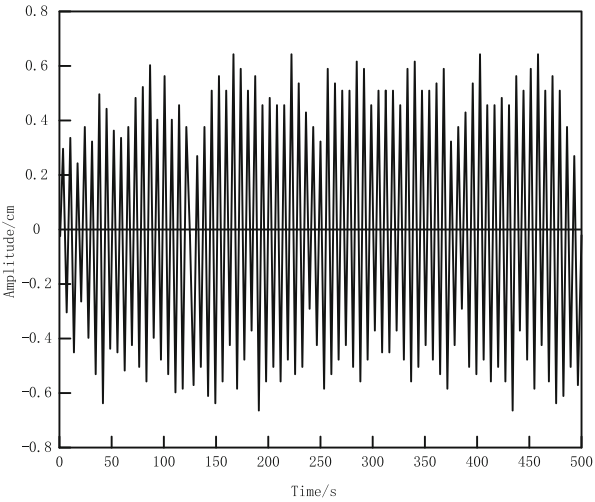

Fig. 3. Sampling of fault data of airborne ocean radar

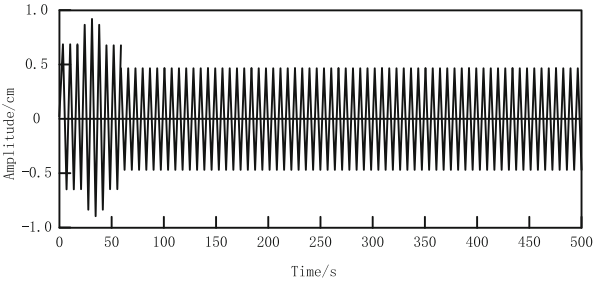

(a) The fusion coefficient is 0.2

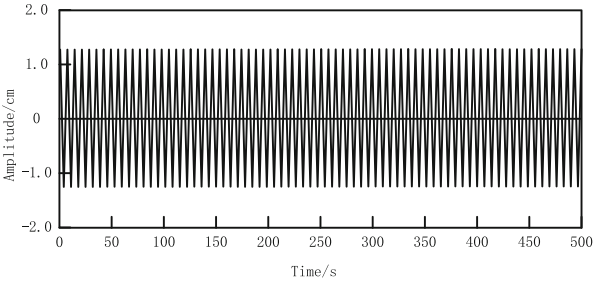

(b) The fusion coefficient is 0.4

Fig. 4. Detection output of airborne ocean radar faults

3.4 Performance Test

The fault detection experiment of airborne ocean radar is carried out in two stages. First, the detection effect of airborne ocean radar faults is measured by using the indicators of missed detection rate and false detection rate. The missed detection rate refers to the

proportion of fault signals not found in the fault detection of airborne ocean radar in the total number of faults. The false detection rate refers to the ratio of detected faults to the total number of airborne ocean radar faults; The signal-to-noise ratio index is used to measure the detection quality of fault signals of airborne ocean radar in the second stage of the experiment. The calculation formula is:

$$SNR = 10 \log \frac{\sum_{i=1}^{N} |a(i)|^2}{\sum_{i=1}^{N} |a(i) - \overline{a}(i)|^2} \tag{28}$$

where, $a(i)$ represents the fault occurrence signal function of airborne ocean radar, $\overline{a}(i)$ represents the signal strength of airborne ocean radar failure, and N represents the number of fault data.

The fault detection method based on PLC technology (literature 3) obtains the frequency band components of the motor by wavelet packet analysis, and extracts the fault characteristic parameters by analysing the changes of each frequency band component. According to the fault characteristics, linear fault information is obtained by using PLC technology and the fault detection is completed by using fuzzy kernel clustering method; the fault detection method based on generation uncertainty (literature 4) uses the random response surface method to obtain the cumulative probability distribution of the load margin under fault conditions, filter and sort out the static voltage stability and complete the fault detection. In order to verify the advantages of the method in this paper, the above two traditional methods based on PLC technology (Ref. 3) and the fault detection method based on generation uncertainty (Ref. 4) were used as comparison methods and tested against the method in this paper. The data samples in Fig. 3 were used to test the fault miss rate of the three methods for airborne marine radar. The results are displayed in Fig. 5.

It can be seen that the fault detection method based on PLC technology has a high missed detection rate when detecting the faults of airborne ocean radar from the results in Fig. 5. When the amount of fault data exceeds 60, the missed detection rate is as high as 57%. As the amount of data increases, the maximum missed detection rate reaches 70%; when the fault detection method based on the uncertainty of power generation is used, the fault missed detection rate is low, between 0 and 40%, which is significantly lower than that based on PLC technology. For the fault detection method, when the method in this paper is adopted, when the amount of fault data is 50, the fault missed detection rate reaches the maximum value of 10%. The missed detection rate begins to decrease, indicating that the judgment of the fault area can be accurate with the increase of the fault data volume. Locate the location of the fault, reducing the missed detection rate.

The test results of the fault detection rate of airborne ocean radar are shown in Fig. 6.

It can be seen from the results in Fig. 6 that the test results of the fault detection method based on PLC technology and the fault detection method based on the uncertainty of power generation in terms of the fault error detection rate of airborne ocean radar are relatively high, ranging from 0 to 75% and 0 to 40% respectively, while the error detection rate of the method in this paper in detecting the fault of airborne ocean radar is between

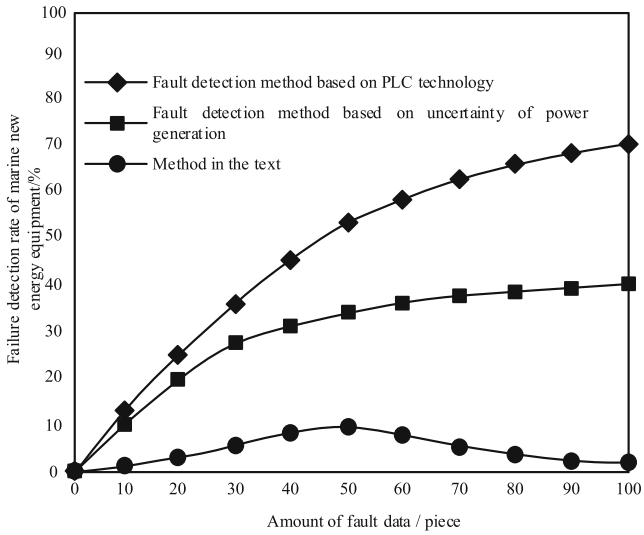

Fig. 5. The test results of the failure and missed detection rate of airborne ocean radar

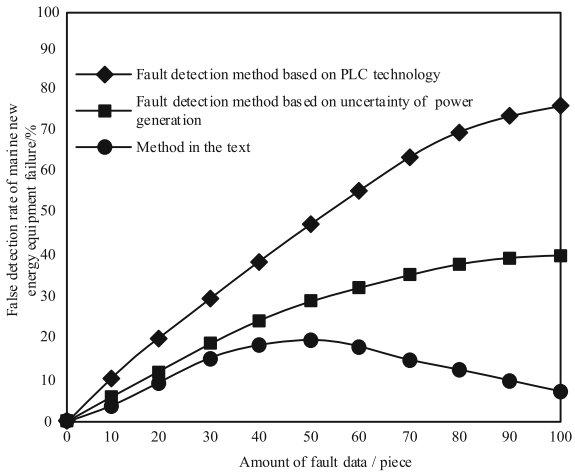

Fig. 6. Test results of fault detection rate of airborne ocean radar

0 and 20%. When the amount of fault data exceeds 50, the fault error detection rate starts to gradually decrease, When the amount of fault data is 100, the fault false detection rate is only 8%. It is stated that the method in the text can avoid the phenomenon of false detection of airborne ocean radar faults.

The results of the marine radar fault message recognition rate comparison test are shown in Fig. 7.

From the results in Fig. 7, it can be seen that the above two traditional methods based on PLC technology (Ref. 3) and the fault detection method based on generation

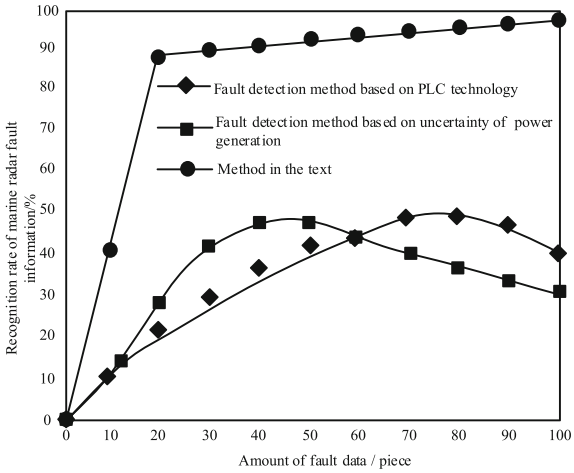

Fig. 7. Marine radar fault message recognition test results

uncertainty (Ref. 4) both The fault information recognition rate of both traditional methods is below 50%, and the information recognition effect is poor and cannot effectively locate the faulty equipment. When the number of fault data exceeds 30, the recognition rate of this method is above 90%, and when the number of data is 100, the recognition rate of this method is as high as 98%. The main reason is that this paper's method uses wavelet transform to transform the fault information, which can accurately locate the faulty marine radar, therefore, the fault information recognition rate is high.

The signal-to-noise ratio test results of the three methods in the fault signal collection of airborne ocean radar are shown in Fig. 8.

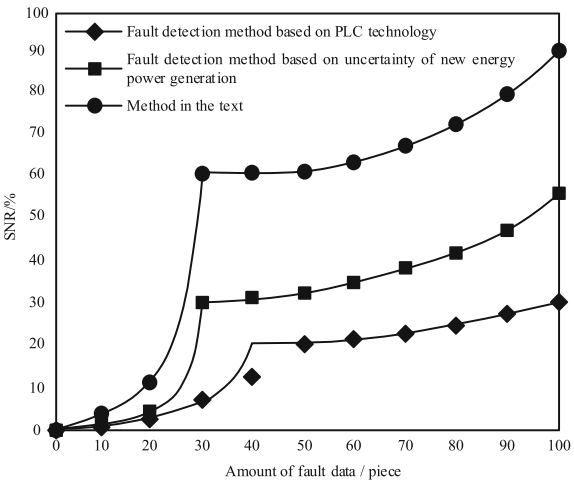

Fig. 8. SNR test results

It can be seen from the results in Fig. 8 that in the signal-to-noise ratio test of collecting fault signals of airborne ocean radar, when the amount of fault data exceeds 40, the fault detection method based on PLC technology reaches 20% signal-to-noise ratio. When the amount of fault data exceeds 30, the signal-to-noise ratio obtained by the fault detection method based on the uncertainty of power generation and the method in the paper reaches 30% and 60%. The signal-to-noise ratio of the method in this paper is still rising rapidly when collecting fault signals of airborne ocean radar with the increase of the amount of fault data. When the amount of fault data exceeds 100, the signal-to-noise ratio of the collected fault signals of airborne ocean radar is as high as 90%. This method utilizes the operating trajectories of fault data variables at different times to detect airborne marine radar faults and extract key variable information for detection. It can effectively ensure the detection quality of airborne marine radar fault signals.

4 Conclusion

A fault detection algorithm is proposed and improved for ocean radar faults. This algorithm innovatively combines feature extraction algorithms to preprocess fault data, define the feature matching degree of fault data, calculate the average trajectory of the working state observation vector, and combine the operation trajectory of fault data variables at different times to detect faults in marine radar, achieving efficient fault detection. The example analysis results show that the algorithm has good performance in fault detection of ocean radar. However, there are still many shortcomings in this study, and it is hoped that engineering case studies can be conducted in future research. Under on-site working conditions, the impact of noise factors on the operation of marine radar can be eliminated, and the working status of marine radar can be obtained. This helps marine survey personnel to timely detect radar equipment faults and accurately locate and diagnose problems. Based on this, potential fault problems can be identified in a timely manner, improving the safety of marine traffic, and ensuring the efficiency and accuracy of marine sub resource survey.

Acknowledgement. 2020 Teaching Research Project of Wuhan Institute of Design and Sciences: Case based “linear algebra” Hybrid Teaching Research and Practice (Project No.: 2020JY101).

References

1. Akta, A., Kriek, Y.: A novel optimal energy management strategy for offshore wind/marine current/battery/ultracapacitor hybrid renewable energy system. Energy **199**(15), 117425–117438 (2020)
2. Ren, Y., Huang, J., Hu, L., et al.: Denoising algorithm of hydro-generator set based on fourier decomposition and permutation entropy. Water Power **46**(10), 96–99+116 (2020)
3. Wang, L., Wang, Y., Zhang, Y.: Fault detection of new energy vehicle motor drive system based on PLC technology. Mach. Des. Manuf. 06, 199–202+207 (2022)
4. Haibo, B.A.O., Xiaoxuan, G.U.O.: Fault screening and ranking method of static voltage stability considering uncertainty of renewable energy power generation. Electr. Power Autom. Equipment **39**(7), 57–63 (2019)

5. Wumaier,·T., Mu, H., Xia, Q.: Vibrationfault diagnosis of water turbine-generator set based on artificial immune algorithm. Yangtze River **52**(5), 209–211+222 (2021)
6. Jia, Q., Guo, J., Sheng, B.: Research on pattern recognition of LiDAR hardware fault data. Laser J. **43**(4), 195–199 (2022)
7. Chen, J., Xu, H., Wu, T.: Fault early warning technology of airborne radar based on wavelet energy spectrum entropy and HMM. Fire Control Command Control **47**(10):31–35+40
8. Bian, H.U., Picheng, T.A.N., Yuan, Y.E., et al.: Design of noise signal acquisition system for bulb tubular hydro-generating unit based on acoustic characteristics. Chin. Meas. Test **47**(03), 139–143 (2021)
9. Silva, A., Zarzo, A., González, J.M.M., Munoz-Guijosa, J.M.: Early fault detection of single-point rub in gas turbines with accelerometers on the casing based on continuous wavelet transform. J. Sound Vib. **487**(10), 460–480 (2020)
10. Zhang, C., Liu, Y.: Multi-faults diagnosis of rolling bearings via adaptive customization of flexible analytical wavelet bases. Chin. J. Aeronaut. **33**(2), 407–417 (2020)
11. Zhao, J., Hou, H., Gao, Y., et al.: Single-phase ground fault location method for distribution network based on traveling wave time-frequency characteristics. Electr. Power Syst. Res. **186**(Sep.), 106401.1–106401.9 (2020)
12. Zhang, H., Xie, Y., Yi T., et al.: Fault detection for high-voltage circuit breakers based on time-frequency analysis of switching transient e-fields. IEEE Trans. Instrum. Meas. **69**(4 Pt.2), 1620–1631 (2020)